NASr-21(02)

GPO PRICE $ ______

CFSTI PRICE(S) $ ______

Hard copy (HC) $2.00

Microfiche (MF) $ .50

ff 653 July 65

MEMORANDUM
RM-4894-NASA
FEBRUARY 1966

EARTH COVERAGE PATTERNS WITH HIGH-GAIN ANTENNAS ON STATIONARY SATELLITES

W. Sollfrey

PREPARED FOR:
NATIONAL AERONAUTICS AND SPACE ADMINISTRATION

The RAND Corporation
SANTA MONICA • CALIFORNIA

NASr-21(02)

MEMORANDUM
RM-4894-NASA
FEBRUARY 1966

EARTH COVERAGE PATTERNS WITH HIGH-GAIN ANTENNAS ON STATIONARY SATELLITES

W. Sollfrey

N66-21823

This research is sponsored by the National Aeronautics and Space Administration under Contract No. NASr-21. This report does not necessarily represent the views of the National Aeronautics and Space Administration.

The RAND Corporation
1700 MAIN ST. • SANTA MONICA • CALIFORNIA • 90406

Published by The RAND Corporation

PREFACE

This Memorandum is part of RAND's continuing study of Communications Satellite Technology for the National Aeronautics and Space Administration. It presents coverage patterns which may be attained by the use of highly directive antennas on stationary communications satellites. As constructed, the Memorandum provides a tool for the interested reader, who may use it to investigate antenna patterns for satellites at various locations. A typical application would be a 7° beamwidth antenna on a satellite at 58° W longitude on the equator, looking at a point offset 45° at an azimuth of 75° north of east. This antenna has about 28 db of gain, and the configuration could be used for air traffic control over the entire North Atlantic region. Other patterns of significant application may be found by using the coverage charts and overlay map provided.

21827

SUMMARY

This Memorandum presents coverage patterns which may be attained by the use of highly directive antennas on stationary communications satellites. The equations for the intersection of a sphere and a conical beam aimed at an arbitrary point on the sphere are set up and solved. The results are presented in graphic form. Coverage patterns are plotted on Mercator charts for antennas of 2° to 10° beamwidth aimed at points on the earth's surface offset from the subsatellite point by 0, 30, 45, and 60 great-circle degrees at various antenna azimuths. An overlay Mercator map of the earth is provided, which permits the user to find the effect of placing the satellite at different longitudes along the equator.

As a typical result of the use of these curves, it has been found that the North Atlantic region can be covered from a satellite with a 7° antenna beamwidth at 58° W longitude looking at a point offset 45° with an azimuth of 75° north of east. The entire region visible to a synchronous satellite may be covered by a 17° beamwidth. Thus, a 7.7-db increase in antenna gain is available. The curves and overlay map permit the reader to find other possibilities.

Author

CONTENTS

LIST OF FIGURES

I. INTRODUCTION

The present generation of synchronous satellites (Syncom, Early Bird) employs antennas with only moderate directivity. This situation has three causes: spin-stabilization, limited payload, and desire to achieve as great an earth coverage as possible. Future synchronous satellites (ATS) may employ gravity-gradient or other stabilization schemes, and enhanced payload capability may permit the use of larger antennas. Therefore, it is of interest to study the coverage patterns which highly directive antennas will present on the earth's surface.

In Section II, the equations for the intersection of a conical antenna beam and the earth's surface are set up and solved. In Section III, the results are presented in graphic form, in a manner which should permit the interested reader to use this Memorandum as a tool for further investigations. The coverage patterns for antennas of 2° to 10° beamwidth, aimed at points on the earth's surface offset by 0, 30, 45, and 60 great-circle degrees from the subsatellite point, are given for various antenna azimuths. These are plotted on Mercator charts. A Mercator map of the earth is provided, which permits the user to find the effect of placing the satellite at different longitudes along the equator.

As demonstrations of the utility of these curves, it has been found that the entire North Atlantic region can be covered with a beamwidth of 7°, using a satellite at 58° W longitude looking at a point offset 45° at an azimuth of 75° (0° azimuth is due east). This could be used for air traffic control. All of Europe can be covered from a satellite at 10° E longitude with a 4° beamwidth looking at a point offset 45° due north. All of East Asia (India to Indonesia to Japan) can be covered from a satellite at 152° E with a 9° beam looking at a point offset 30° with an azimuth of 150°. The North Pacific region--Japan, Hawaii, Alaska, U.S. (San Francisco)--can be covered from a satellite at 165° E with a 10° beam looking at a point offset 45° at an azimuth of 75°. If the India ground station were at Calcutta, this 165° E satellite could cover both the North Pacific and East Asia regions with two antennas. Other possibilities may be found by the reader. The entire region visible to a synchronous satellite may be covered by a 17° beamwidth and corresponding antenna gain of 20 db. These investigations show that suitable pointing permits roughly halving the beamwidth for plausible coverage regions, with an attendant antenna gain increase of 6 db.

II. ANALYSIS

The analytical problem divides itself into two natural parts. The first is to find the locus of the intersection of a cone and a sphere. The second is to reference that locus to the earth. These will be done in sequence.

The configuration is shown in Fig. 1. The satellite is at point Q on the equatorial plane at height h. The rectangular coordinates X, Y, Z are so oriented that P is due "north" of the subsatellite point. The antenna is aimed at point P, which is offset from the subsatellite point by the angle β. Visualization shows that the shape of the intersection curve is invariant with respect to a rotation of the beam around the line joining the satellite to the center of the earth, which will be taken as the X-axis. This invariance is depicted in Fig. 2, which shows the projection of the intersection curve into the Y_E-Z_E plane, where the coordinates X_E, Y_E, Z_E are earth-oriented. The shape of the projected curve does not depend on the azimuth angle θ, but only on the distance from the center. The line PQ will lie in the X-Z plane, and the aiming point P projects onto the Z-axis in Fig. 2. The cone, of semiangle α, will intersect the sphere in a curve whose equation is to be found.

Introduce auxiliary coordinates X', Z', lying in the X-Z plane, with the X'-axis along the line PQ and the Z'-axis passing through the center of the sphere, as shown in Fig. 1. The angle γ, which measures the deflection of the antenna axis from the subsatellite point, may be found by applying the law of sines to the triangle OPQ.

Thus

$$\frac{r}{\sin \gamma} = \frac{r + h}{\sin(\pi-\beta-\gamma)} = \frac{r + h}{\sin(\beta+\gamma)} \tag{1}$$

Define the parameter k as the satellite radial distance in units of the earth's radius, so

$$k = \frac{r + h}{r} \tag{2}$$

For a synchronous satellite at an altitude of 19,310 n mi, $k = 6.6134$. The angle γ is now given by

$$\tan \gamma = \frac{\sin \beta}{k - \cos \beta} \tag{3}$$

Use the earth's radius as the unit of distance. The equations connecting the auxiliary coordinates x', z' to the rectangular coordinates x, z are

$$x' = x \cos \gamma - z \sin \gamma \tag{4}$$

$$z' = x \sin \gamma + z \cos \gamma - k \sin \gamma \tag{5}$$

The equation of the line QS, which is a generator of the cone, is given by

$$z' = \tan \alpha(k \cos \gamma - x') \tag{6}$$

This may be seen easily. From the triangle $00'Q$, the distance $0'Q$ is $k \cos \gamma$, which determines the horizontal intercept. The line has the slope $-\tan \alpha$, which establishes Eq. (6).

The cone is defined by the condition that all points on it, at a given axial distance from the apex Q, lie on a circle of radius given by Eq. (6). Squaring and replacing z' by the three dimensional perpendicular distance then gives the equation of the cone as

$$y^2 + z'^2 = \tan^2 \alpha(k \cos \gamma - x')^2 \tag{7}$$

Upon substituting from Eqs. (4) and (5) in Eq. (7), the equation of the cone in the rectangular coordinates x, y, z is

$$\cos^2\alpha\left[y^2+\{z\cos\gamma-(k-x)\sin\gamma\}^2\right] - \sin^2\alpha\left[z\sin\gamma + (k-x)\cos\gamma\right]^2 = 0 \tag{8}$$

Multiplying out and simplifying reduces this to the form

$$y^2\cos^2\alpha + z^2(\cos^2\gamma-\sin^2\alpha)+(k-x)^2(\sin^2\gamma-\sin^2\alpha)-2z(k-x)\cos\gamma\sin\gamma = 0 \tag{9}$$

The points on the surface of the sphere may be specified by their latitude u and longitude v. Measure the longitude from the subsatellite point. Then the surface of the sphere is defined by

$$x = \cos u \cos v \tag{10}$$

$$y = \cos u \sin v \tag{11}$$

$$z = \sin u \tag{12}$$

These expressions may be substituted in Eq. (9) to obtain the locus of the intersection of the sphere and cone. The resulting equation may be rearranged as a quadratic equation for cos u cos v in terms of sin u; thus

$$\cos^2\gamma\cos^2u\cos^2v-2\left[\cos\gamma\sin\gamma\sin u+k(\cos^2\gamma-\cos^2\alpha)\right]\cos u\cos v$$
$$+\sin^2\gamma\sin^2u-\cos^2\alpha+2k\cos\gamma\sin\gamma\sin u+k^2(\cos^2\gamma-\cos^2\alpha)=0 \tag{13}$$

This equation may be solved for cos u cos v. There will be two solutions, one of which represents the intersection ST of the cone and sphere nearer the apex of the cone, as depicted in Fig. 1; the other represents the intersection farther from the apex. The nearer one may be selected by requiring that the latitude reduce to β and the longitude to zero when the cone semiangle α tends to zero. This requirement leads to the choice of the plus sign for the radical which arises from solution by quadratic formula of Eq. (13). The result is

$$\cos v$$
$$=\frac{1}{\cos u\cos^2\gamma}\left[\begin{array}{l}\cos\gamma\sin\gamma\sin u+k(\cos^2\gamma-\cos^2\alpha)\\ +\cos\alpha\{\cos^2\gamma-2k\cos\gamma\sin\gamma\sin u-k^2(\cos^2\gamma-\cos^2\alpha)\}^{\frac{1}{2}}\end{array}\right] \tag{14}$$

This expression gives the shape of the boundary as long as the radical is positive and $|\cos v| \leq 1$. The point T of Fig. 1 corresponds to $v = 0$. Its latitude may be shown to be

$$u_- = \sin^{-1}[k\sin(\gamma-\alpha)] - (\gamma-\alpha) \tag{15}$$

The point S of Fig. 1, which also corresponds to $v = 0$, has the latitude

$$u_+ = \sin^{-1}[k\sin(\gamma+\alpha)] - (\gamma+\alpha) \tag{16}$$

As long as k $\sin(\gamma+\alpha)$ is less than one, the arc sine of Eq. (16) is defined and the intersection locus is a closed curve. If k sin $(\gamma+\alpha)$ exceeds one, the line QS of Fig. 1 does not intersect the sphere. When k $\sin(\gamma+\alpha)$ equals one, the line QS is tangent to the sphere, which defines the horizon limit. For a synchronous satellite at an altitude of 19,310 n mi, this corresponds to $u_+ = 81.3^o$. The horizon is given by the circle such that all points on it are at a ground distance of 81.3^o from the subsatellite point.

With k $\sin(\gamma+\alpha)$ less than one, the radical in Eq. (14) does not vanish. If k $\sin(\gamma+\alpha)$ exceeds one, there will be a value of u, and two corresponding equal and opposite values of v, for which the radical vanishes. These points give the intersection of the locus with the horizon circle. The boundary locus is now completed by the arc of the horizon circle joining the two indicated points.

The variables u and v represent latitude and longitude in the X, Y, Z coordinate system, which has the aiming point offset in the "northerly" direction. It is necessary to refer Eq. (14) to the earth-oriented system X_E, Y_E, Z_E. From Fig. 2, the relation between the coordinate systems is given by a rotation through the angle θ around the X-axis. Thus,

$$X_E = x \tag{17}$$

$$Y_E = y \sin\theta + z \cos\theta \tag{18}$$

$$Z_E = - y \cos\theta + z \sin\theta \tag{19}$$

Introduce the earth latitude L and longitude λ, with the longitude still referenced to the subsatellite point. Then Eqs. (10), (11), (12) and (17), (18), (19) yield

$$\sin L = \sin \theta \sin u - \cos \theta \cos u \sin v \tag{20}$$

$$\tan \lambda = \sin \theta \tan v + \cos \theta \tan u \sec v \tag{21}$$

If the coordinates L_P, λ_P of the aiming point P are specified instead of the offset distance β and the azimuth θ, the latter quantities may be found by inverting Eqs. (20) and (21), yielding

$$\cos \beta = \cos L_P \cos \lambda_P \tag{22}$$

$$\tan \theta = \tan L_P / \sin \lambda_P \tag{23}$$

From Eqs. (14), (20), and (21), the earth-oriented coordinates of the intersection locus may be found. This completes the analytical treatment. The numerical procedure and graphic results are presented in the next section.

III. NUMERICAL PROCEDURE AND GRAPHIC RESULTS

The numerical procedure in handling the equations follows. Select values of L_p and λ_p, then determine β and θ from Eqs. (22) and (23); or select β and θ initially. The latter choice was employed in the actual calculations. The angle γ is found from Eq. (3). Select values of the cone semiangle α. The antenna beamwidth will be 2α. The altitude ratio k is 6.6134 for a synchronous satellite. Determine u_- from Eq. (15). This determines the point T of Fig. 1, which provides the starting point of the coverage pattern. Increment u by a suitable amount (2^o increments were actually used), and determine the two corresponding values of v from Eq. (14). These values of u and v are substituted in Eq. (20) and (21), and the earth coordinates L and λ are found. The incrementation is continued until either the value u_+ is reached, at which the curve closes; or the radical in Eq. (14) vanishes, at which the curve intersects the horizon circle.

This procedure has been programmed using JOSS,* the RAND on-line time-shared computing system. The intersection loci have been obtained for offset angles of 30^o and 45^o with azimuth angles ranging from 0^o to 90^o in 15^o steps. Antenna beamwidths of 2, 4, 6, 8, and 10 deg have been used. In addition, the curves for no offset, and for 60^o offset, 90^o azimuth have been obtained.

It is desired to present the results in a manner as useful to the reader as possible. While the curves could be drawn on earth maps, this would have a disadvantage in that the longitude of the

---

*JOSS is the trademark and service mark of The RAND Corporation for its computer program and services using that program.

satellite would be fixed. If coverage for various satellite longitudes were required, either there would have to be a great profusion of graphs, or an overlay would be necessary. The latter method has been selected. The coverage patterns are drawn on plain graphs, and a mobile earth map is provided. By aligning the map equator with the graph equator, the satellite longitude may be varied by simply sliding the map over the graph to ascertain the position of best coverage.

The earth map employed is drawn in the Mercator projection. Therefore, the graphs have also been drawn on the nonlinear Mercator latitude scale, with the map and graph scale factors equalized. The equation relating the Mercator latitude L_M to the ordinary latitude L is

$$L_M = \log \frac{1 + \sin L}{\cos L} \tag{24}$$

where both L and L_M are in radians and the logarithm is to base e. The Mercator latitude means the number of units of length above or below the equator which correspond to the ordinary latitude L, but the designator on the map is the ordinary latitude. Thus, if the longitude scale factor were 1 in. = 30°, the points on the chart corresponding to an actual latitude of 30° and 60° would be, respectively, 1.049 and 2.515 in. above the equator but would be designated 30° and 60°. All the curves have been drawn using the transformation of Eq. (24), and are presented in Figs. 3-18.

The absolute horizon is given by the 81.3° circle. Another horizon of interest is such that the satellite appears at an elevation angle of 5^{o} when viewed from the ground. This corresponds to a circle of ground arc 76.6^{o}. This "radio horizon" is shown as the dashed line in the figures. Since coverage out to the absolute horizon can be achieved with a beamwidth of 17^{o}, it was deemed worthwhile only to give the contours out to 10^{o} beamwidth. For beamwidths between 10^{o} and 17^{o}, the achievable gain improvement may not warrant the additional complexity in the satellite required to point the antenna.

Some of the possible coverages which have been found using the overlay map and these figures have been listed in the introduction. There is considerable improvement over the 17^{o} system when the ground coverage region is limited and the antenna properly pointed. However, the North Atlantic region is such that a gain increase of 8 db appears to be the best achievable. An all-Europe system can achieve 13 db, but East Asian and Pacific systems can only achieve 5 db. The evaluation of whether these possible improvements are worthwhile will not be considered here.

The curves of Figs. 3-18 and associated overlay map provide a tool for the reader to find other coverage patterns. Equations (14), (20), and (21) may be used to generate other curves by the indicated numerical procedure.

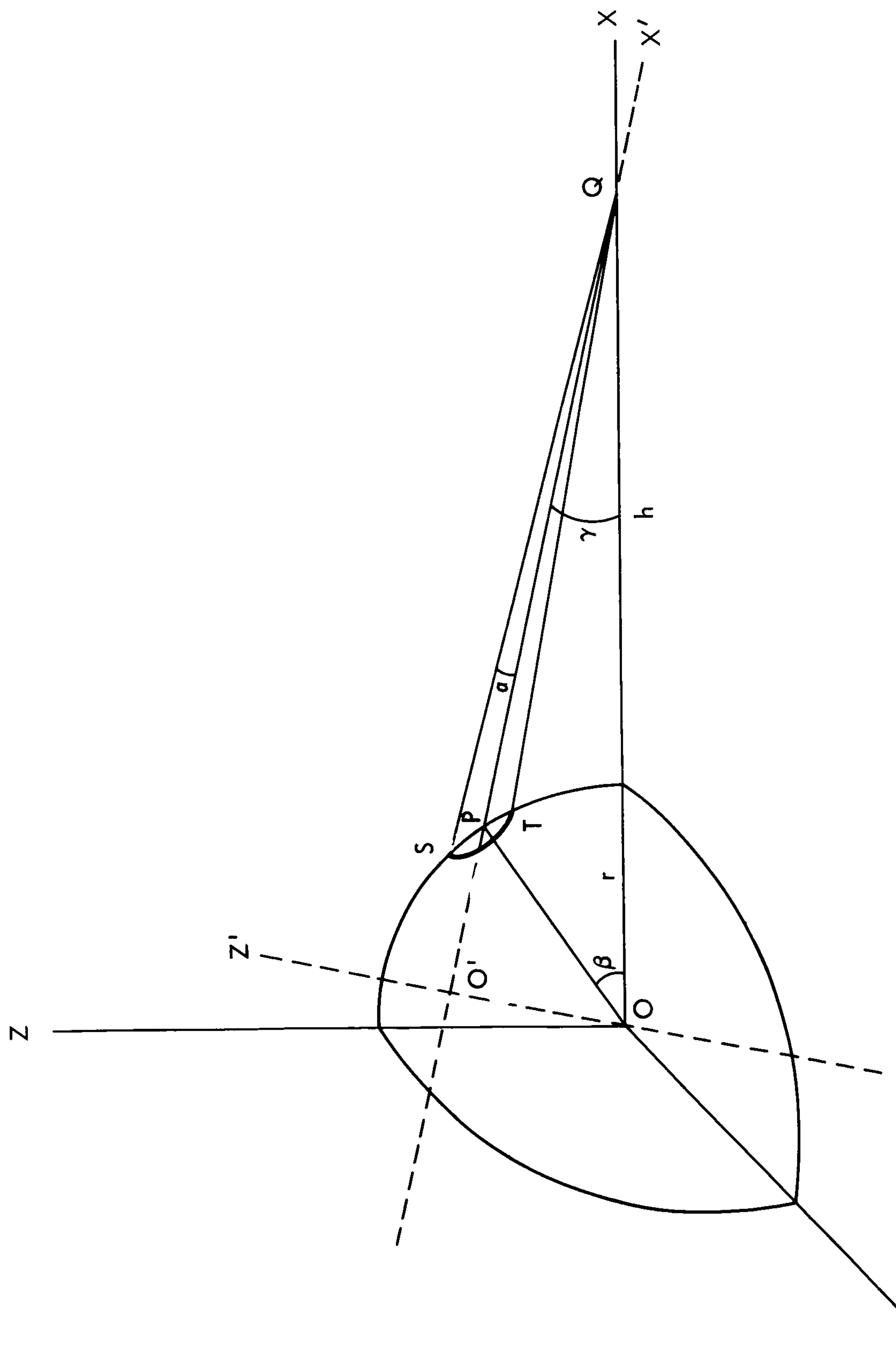

Fig.1—Coordinate system

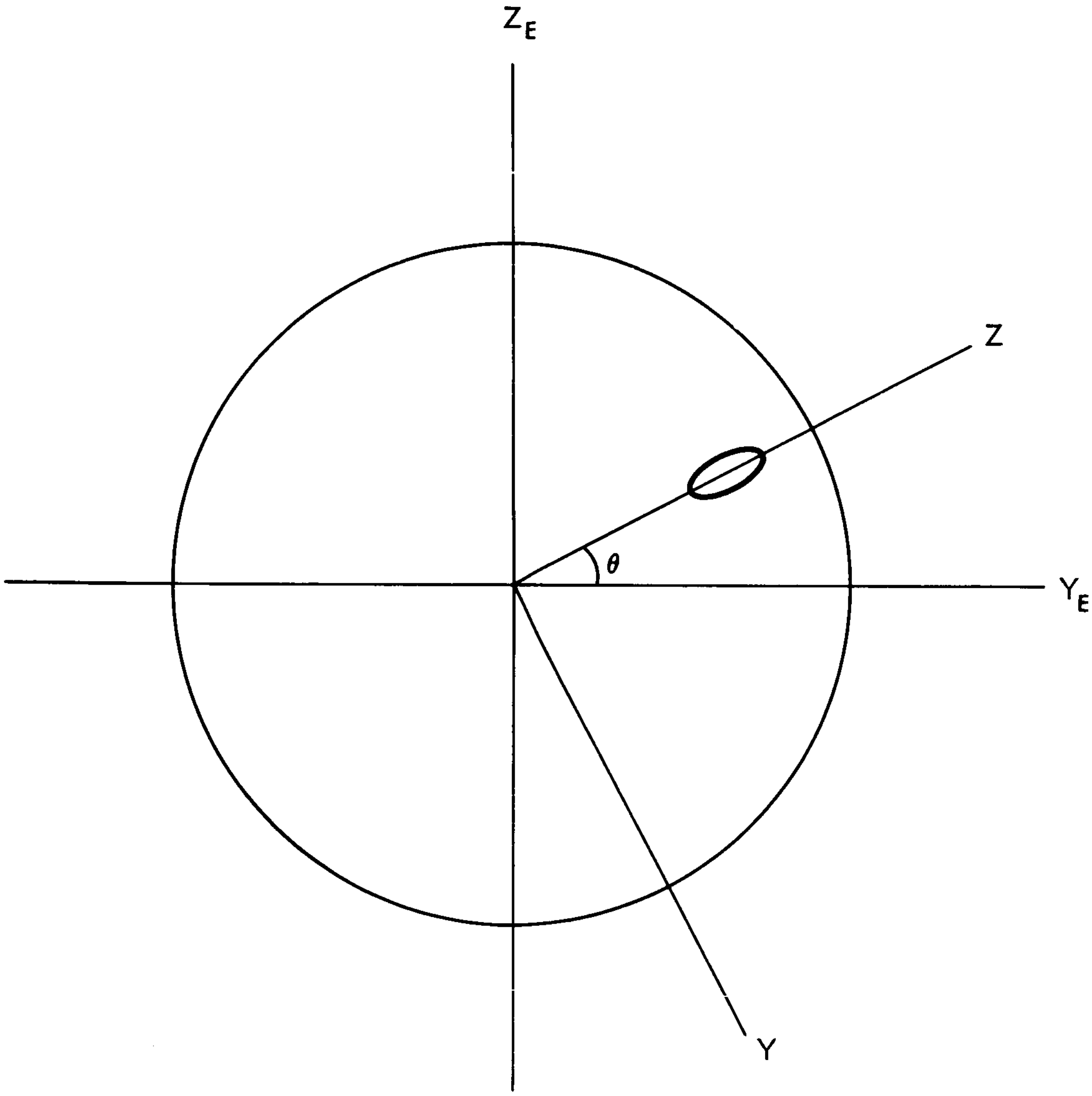

Fig. 2—Projected coordinate system

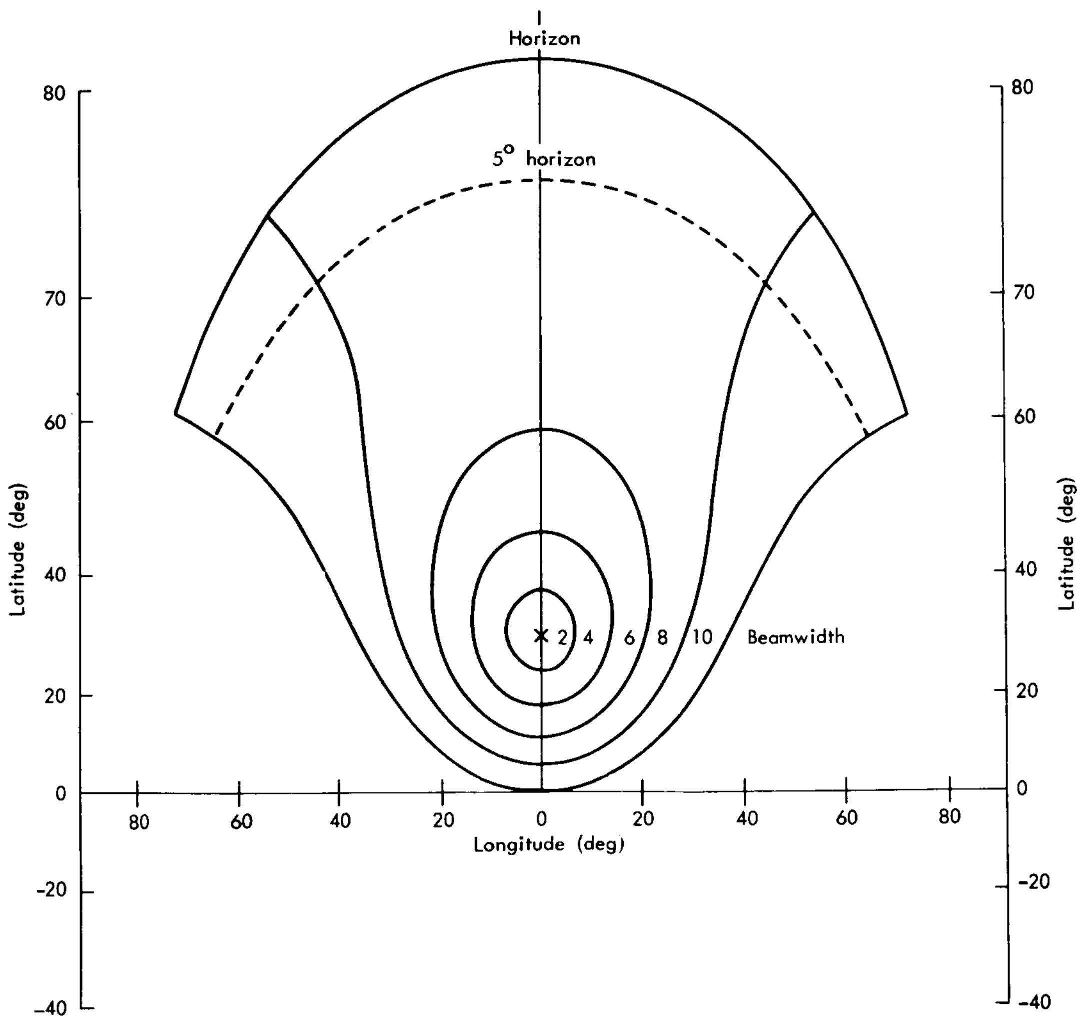

Fig. 3—Earth coverage patterns—offset angle—30°, aximuth—90°

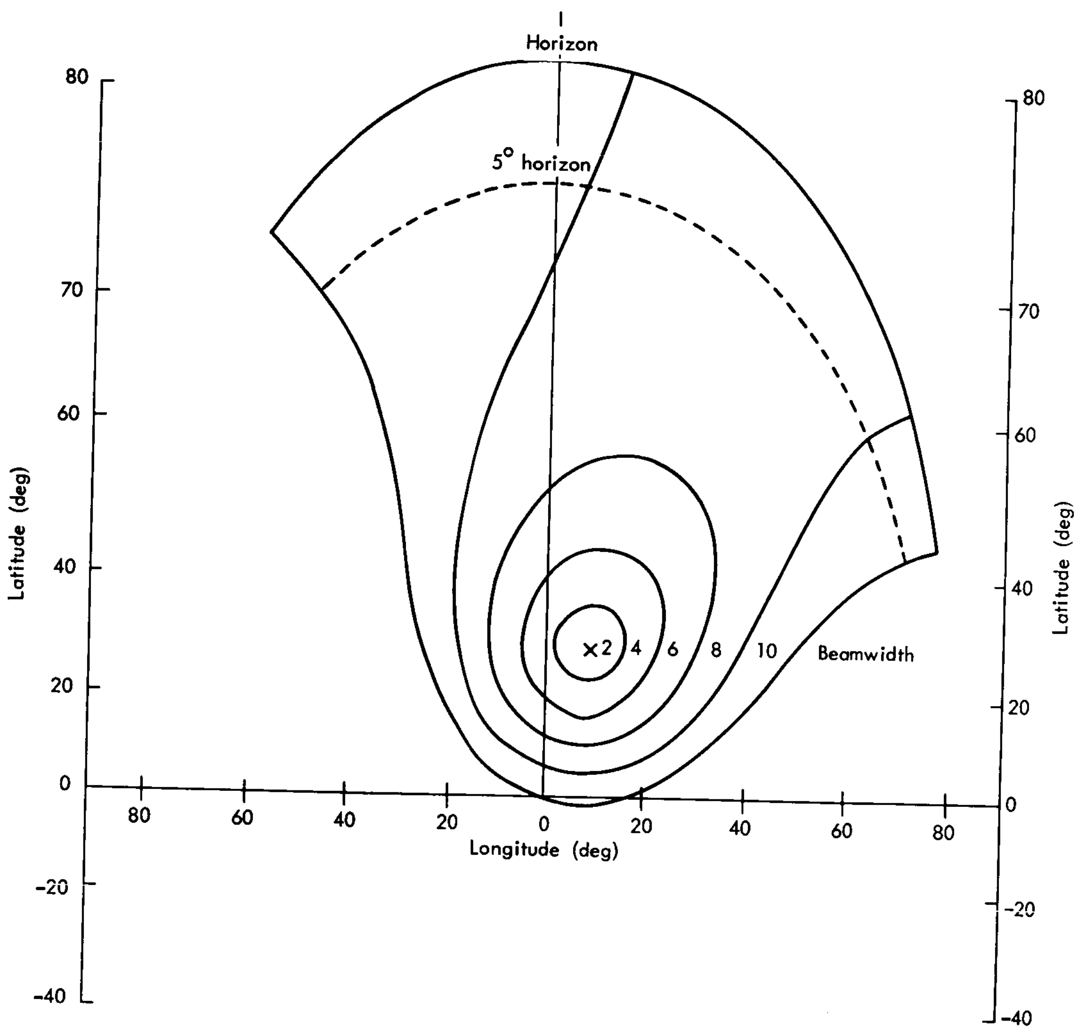

Fig.4—Earth coverage patterns—offset angle—30°, azimuth—75°

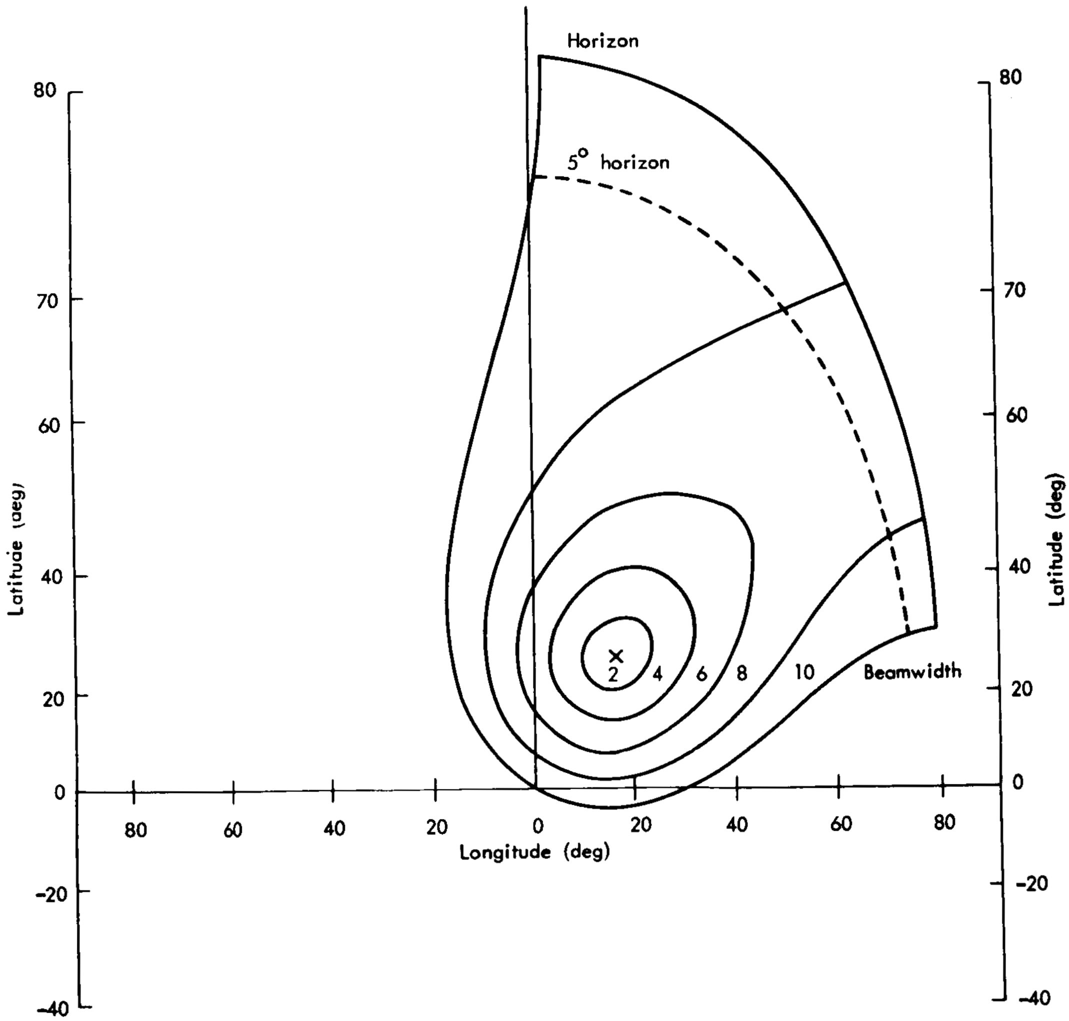

Fig.5—Earth coverage patterns—offset angle—30°, azimuth—60°

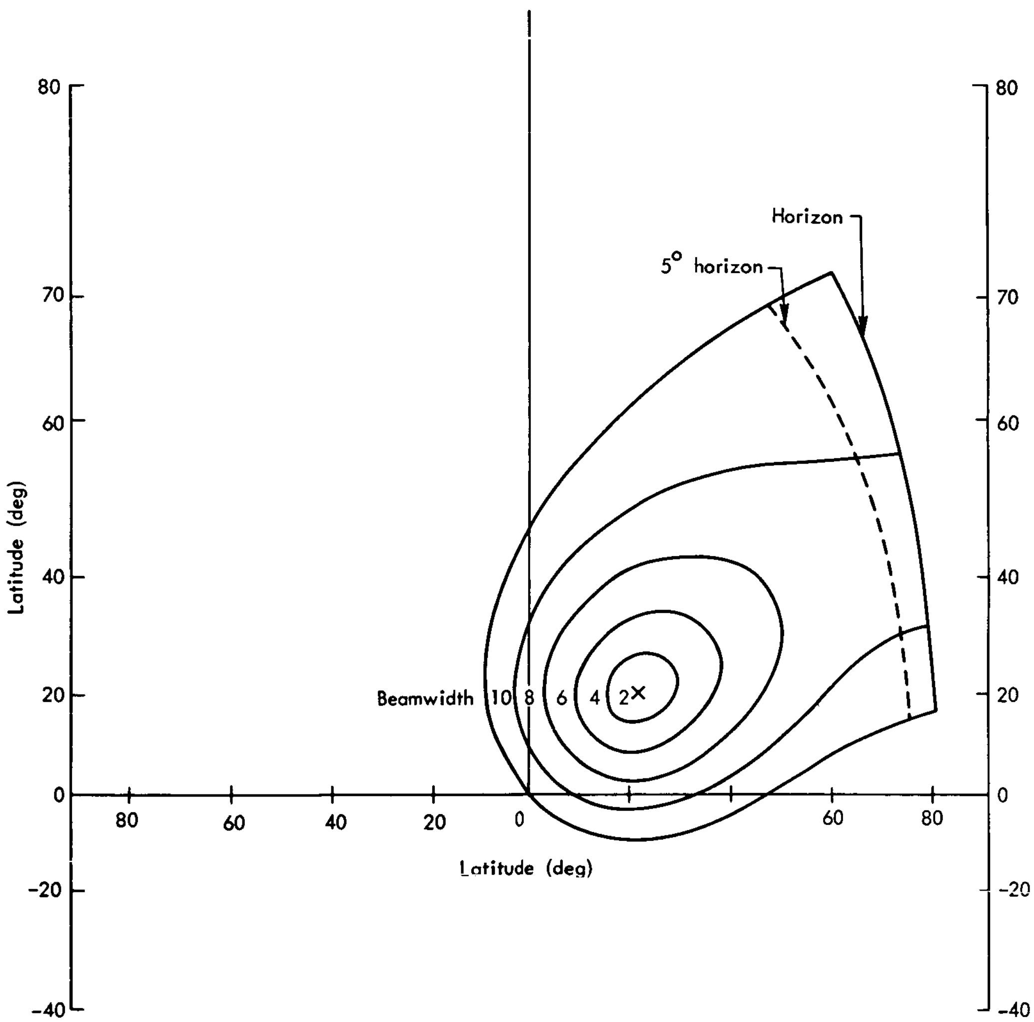

Fig.6—Earth coverage patterns—offset angle—30°, azimuth—45°

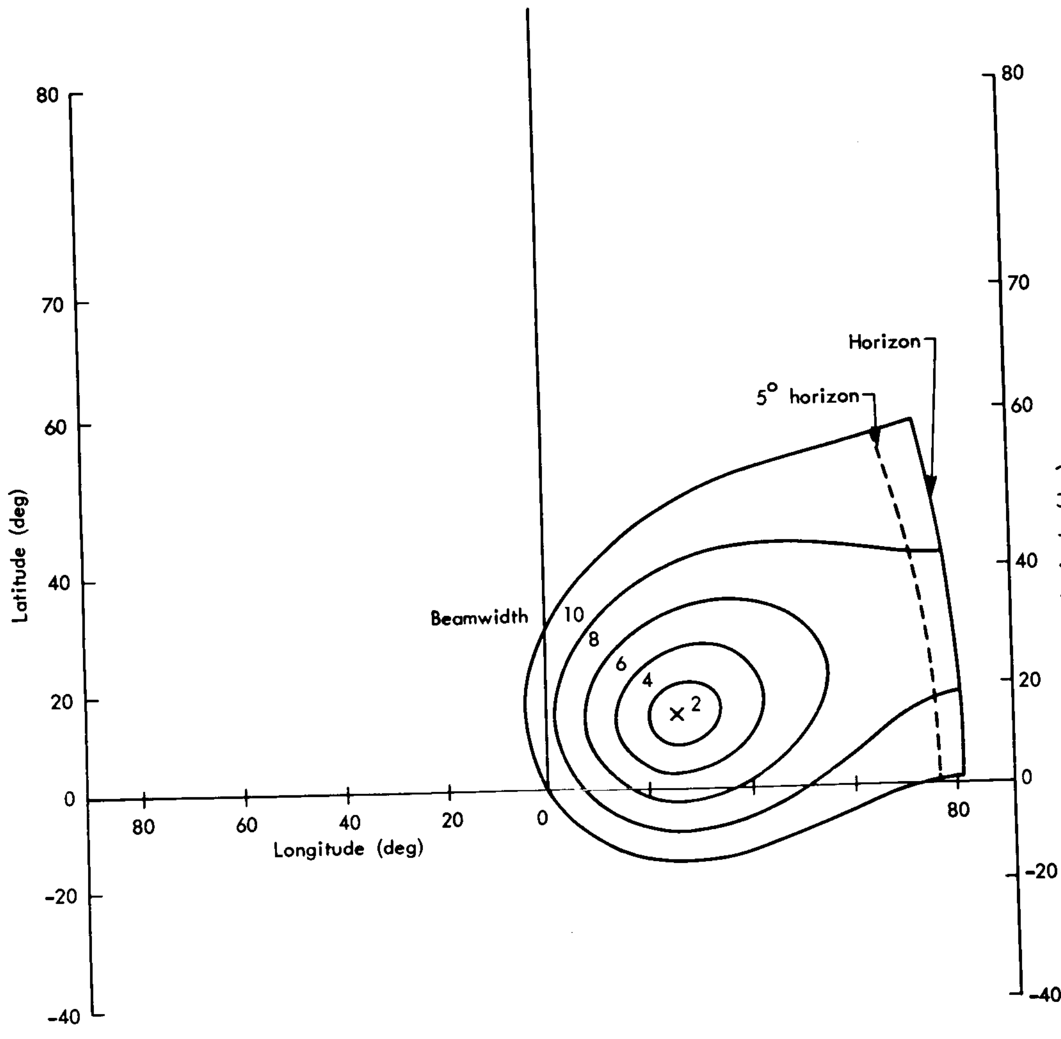

Fig. 7—Earth coverage patterns—offset angle—30°, azimuth—30°

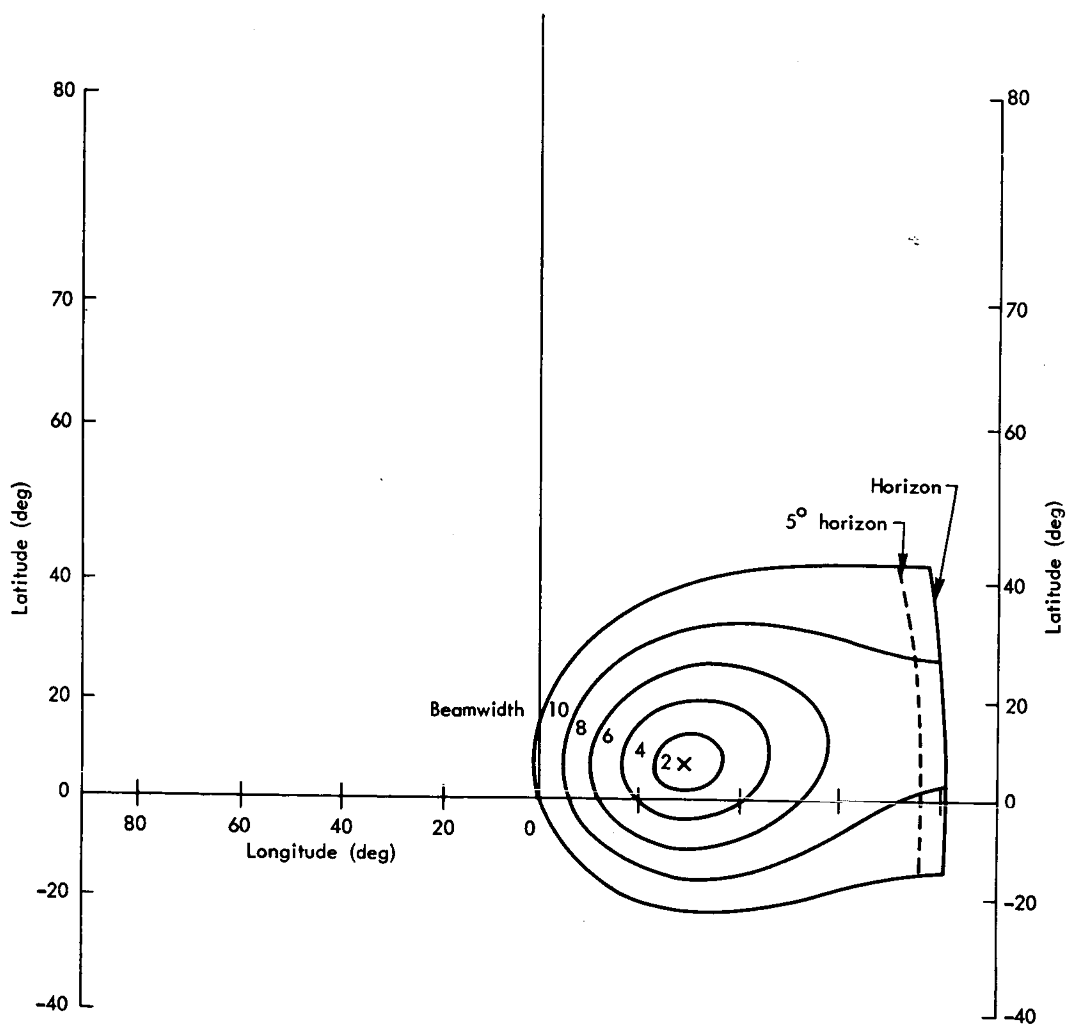

Fig.8—Earth coverage patterns—offset angle—30°, azimuth—15°

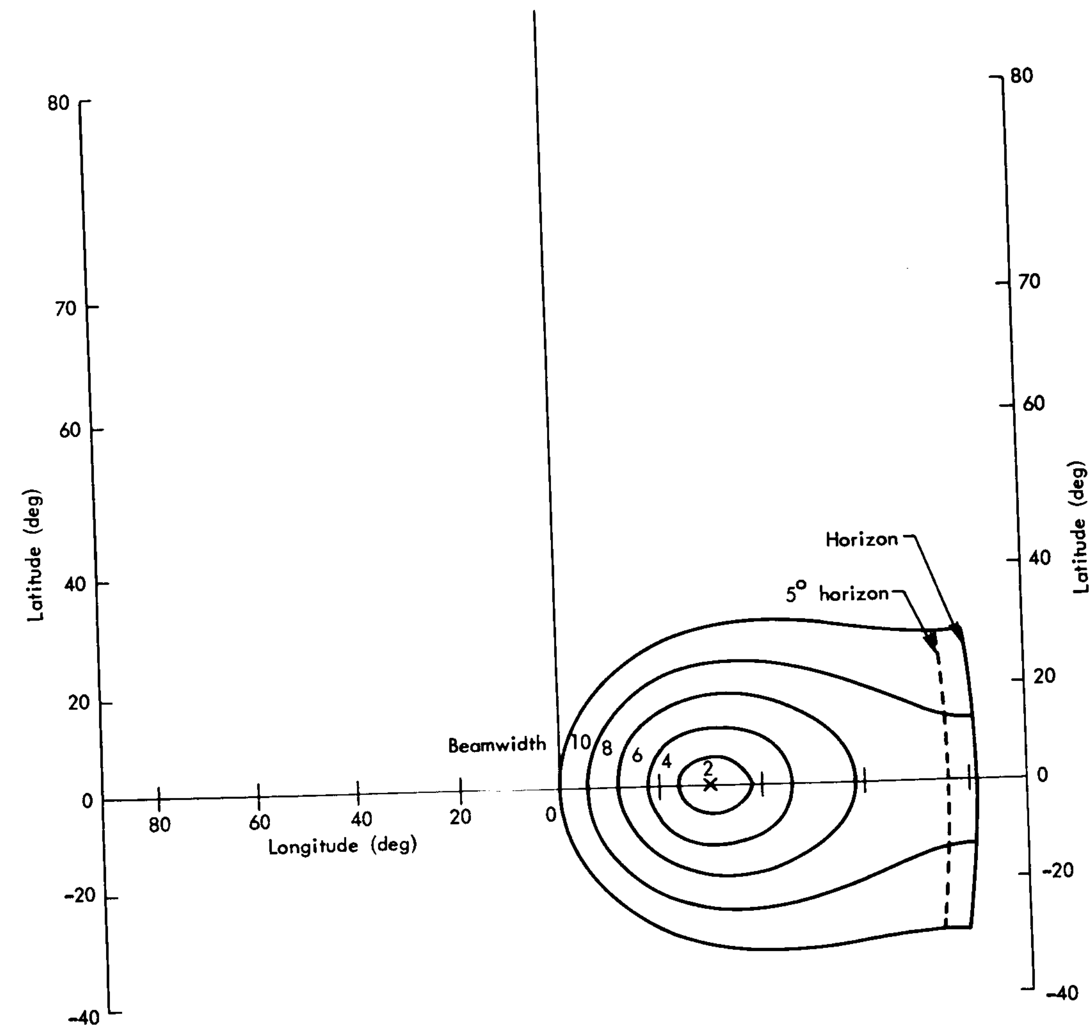

Fig.9—Earth coverage patterns—offset angle—30°, azimuth—0°

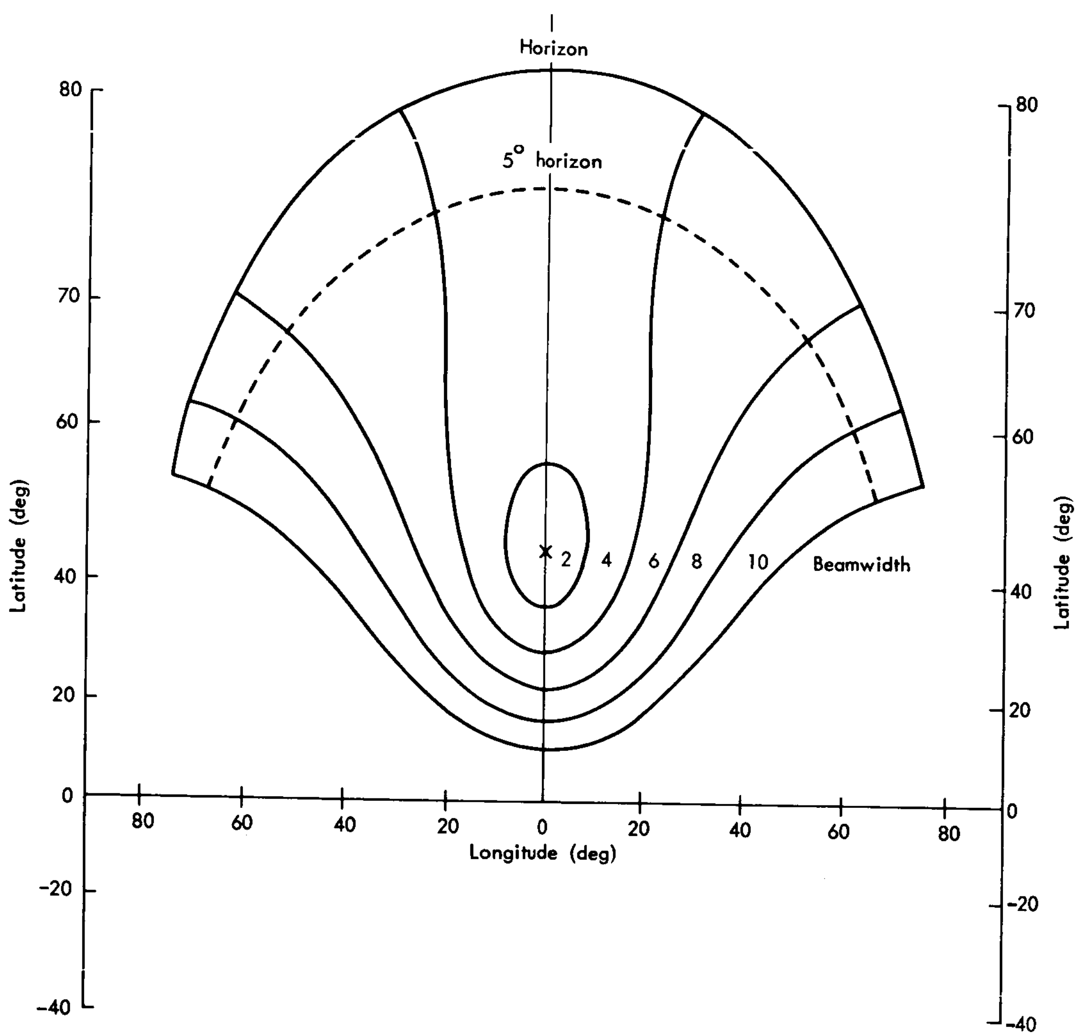

Fig. 10—Earth coverage patterns—offset angle—45°, azimuth—90°

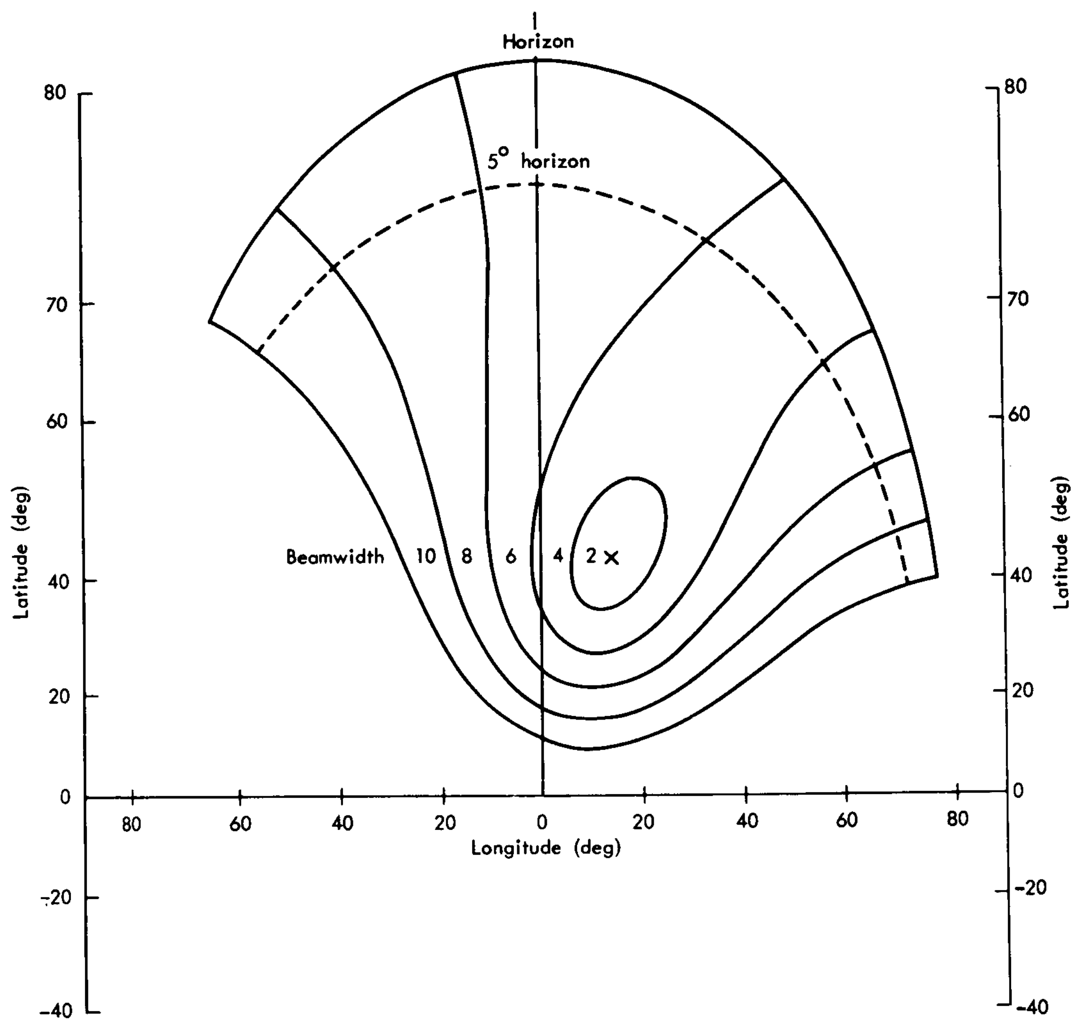

Fig.11—Earth coverage patterns—offset angle—45°, azimuth—75°

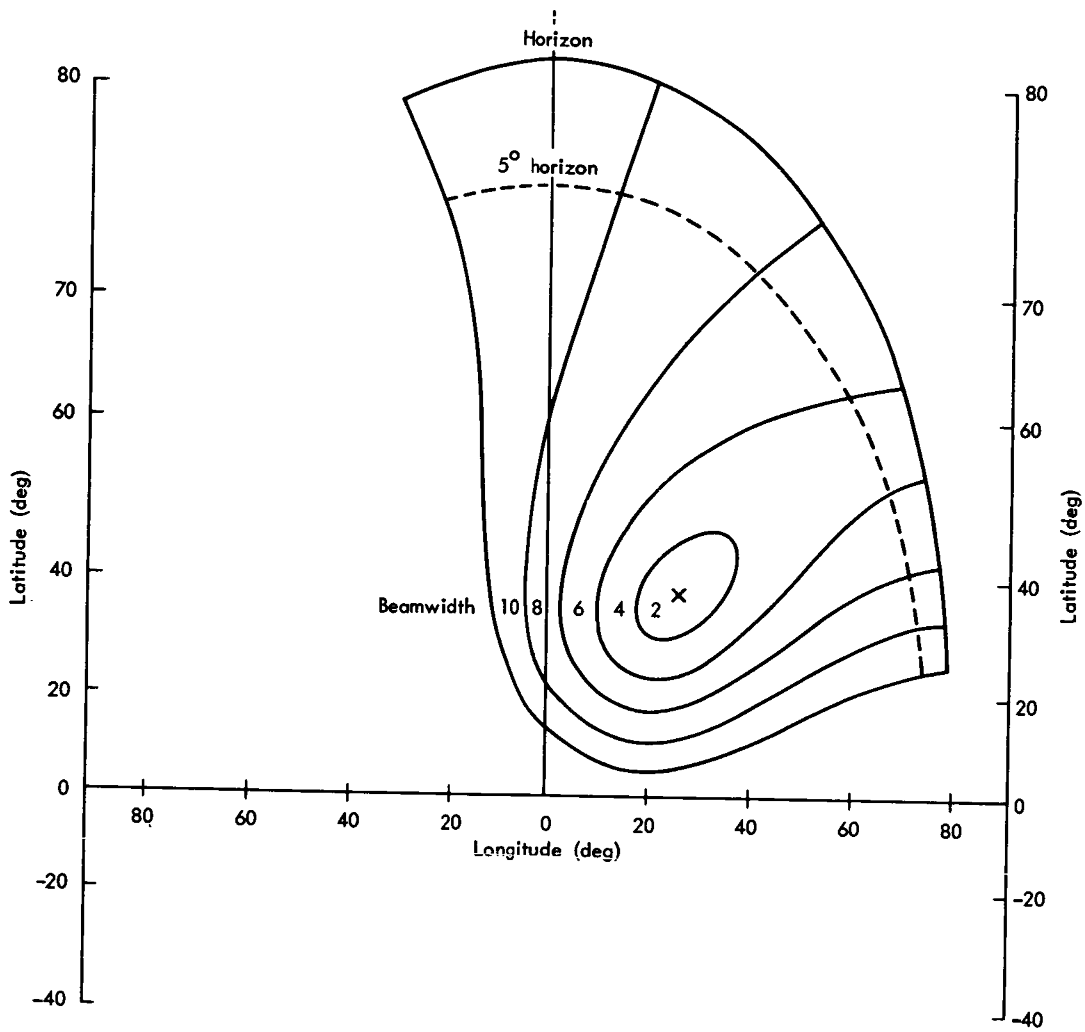

Fig. 12—Earth coverage patterns—offset angle—45°, azimuth—60°

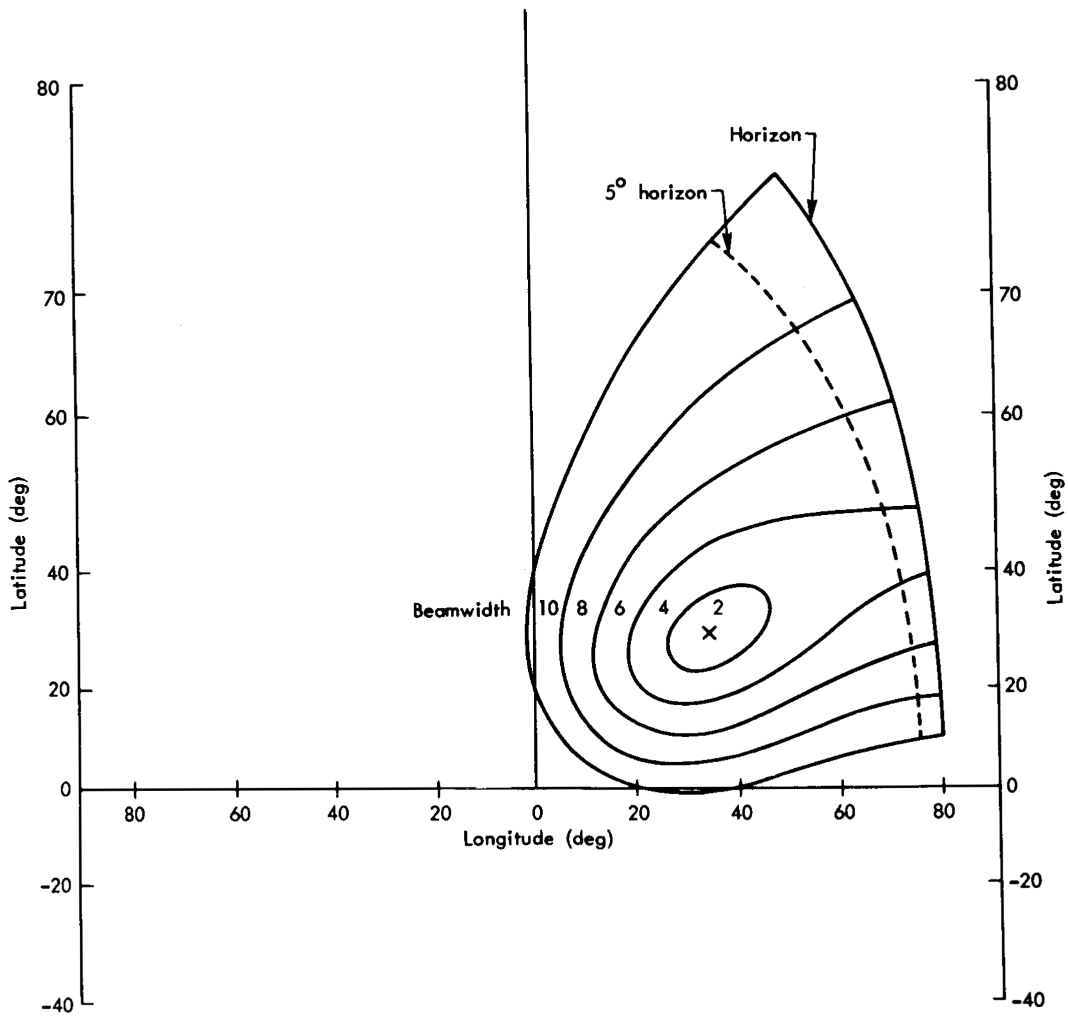

Fig. 13—Earth coverage patterns—offset angle—45°, azimuth—45°

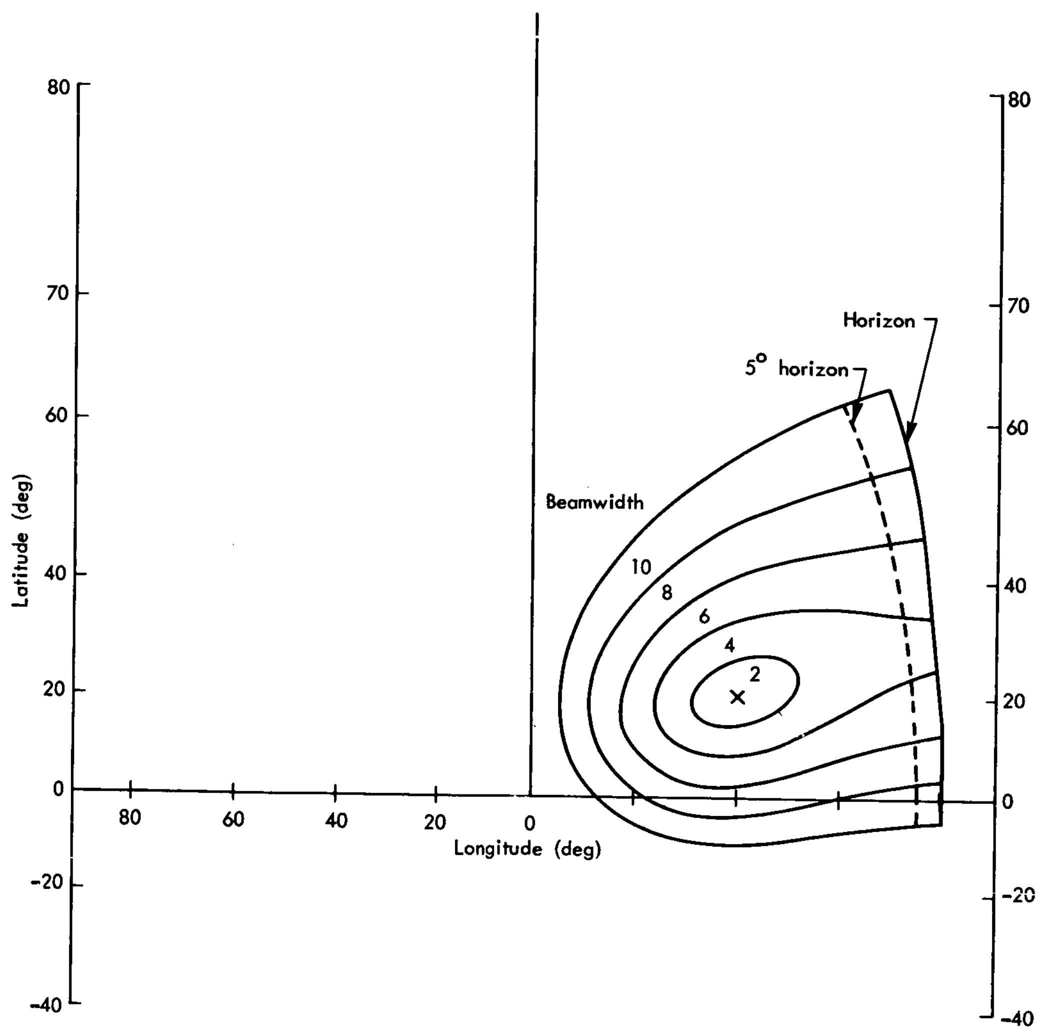

Fig. 14—Earth coverage patterns—offset angle—45°, azimuth—30°

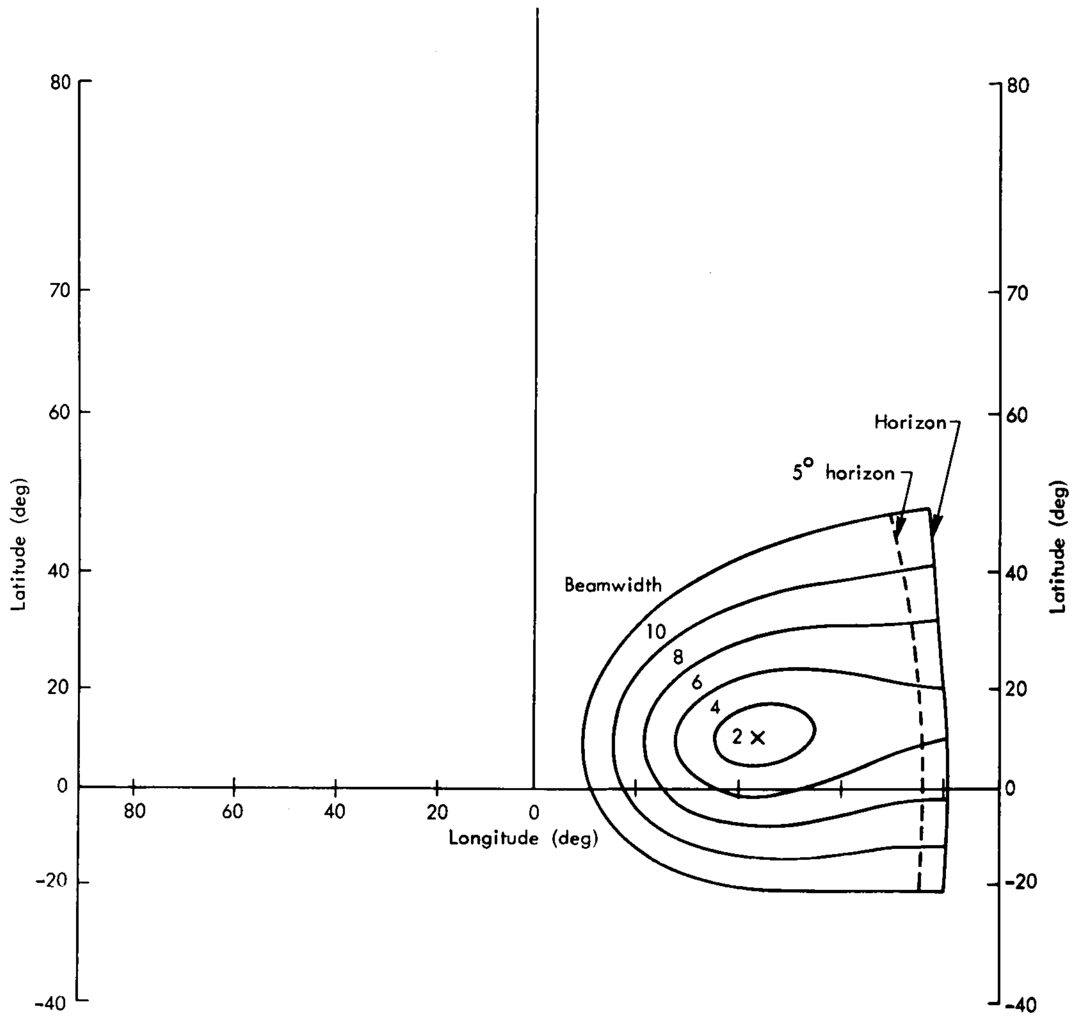

Fig. 15—Earth coverage patterns—offset angle—45°, azimuth—15°

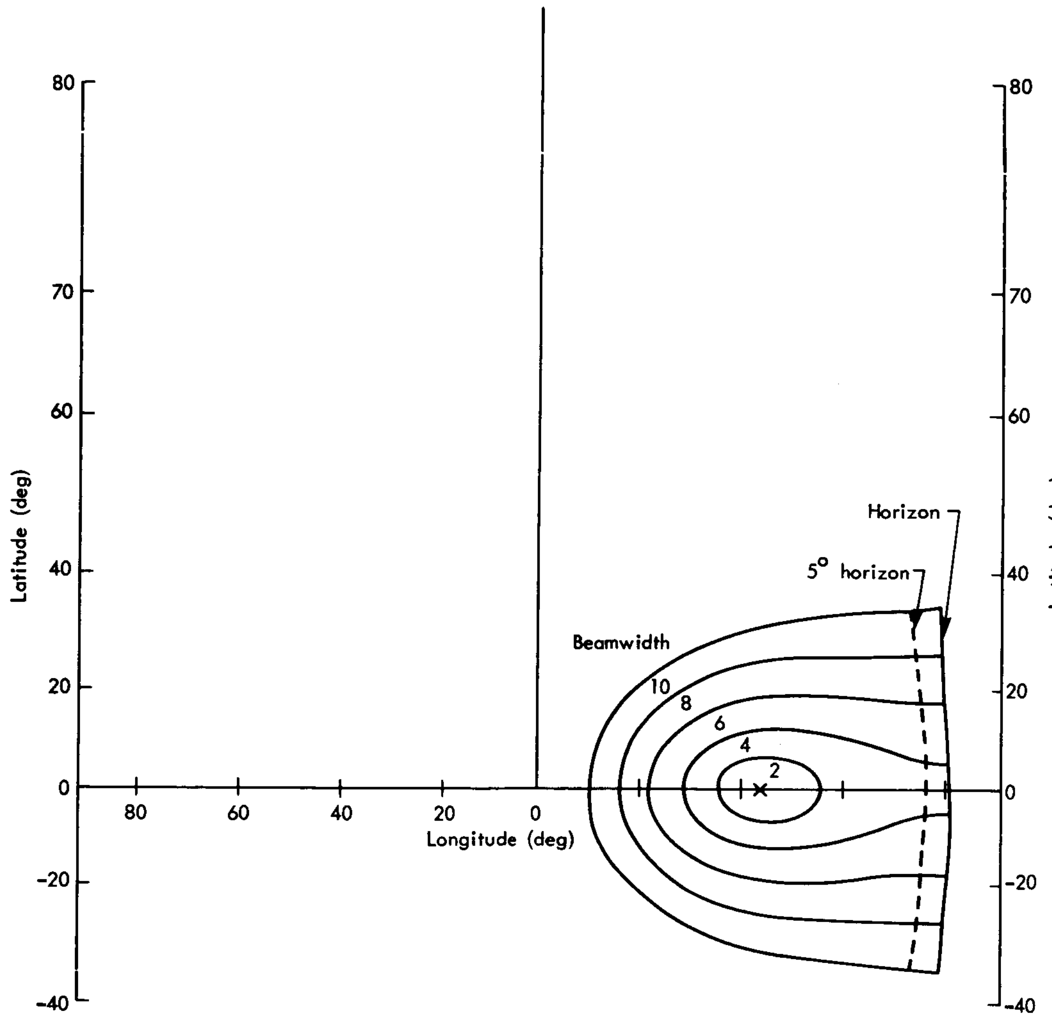

Fig. 16—Earth coverage patterns—offset angle—45°, azimuth—0°

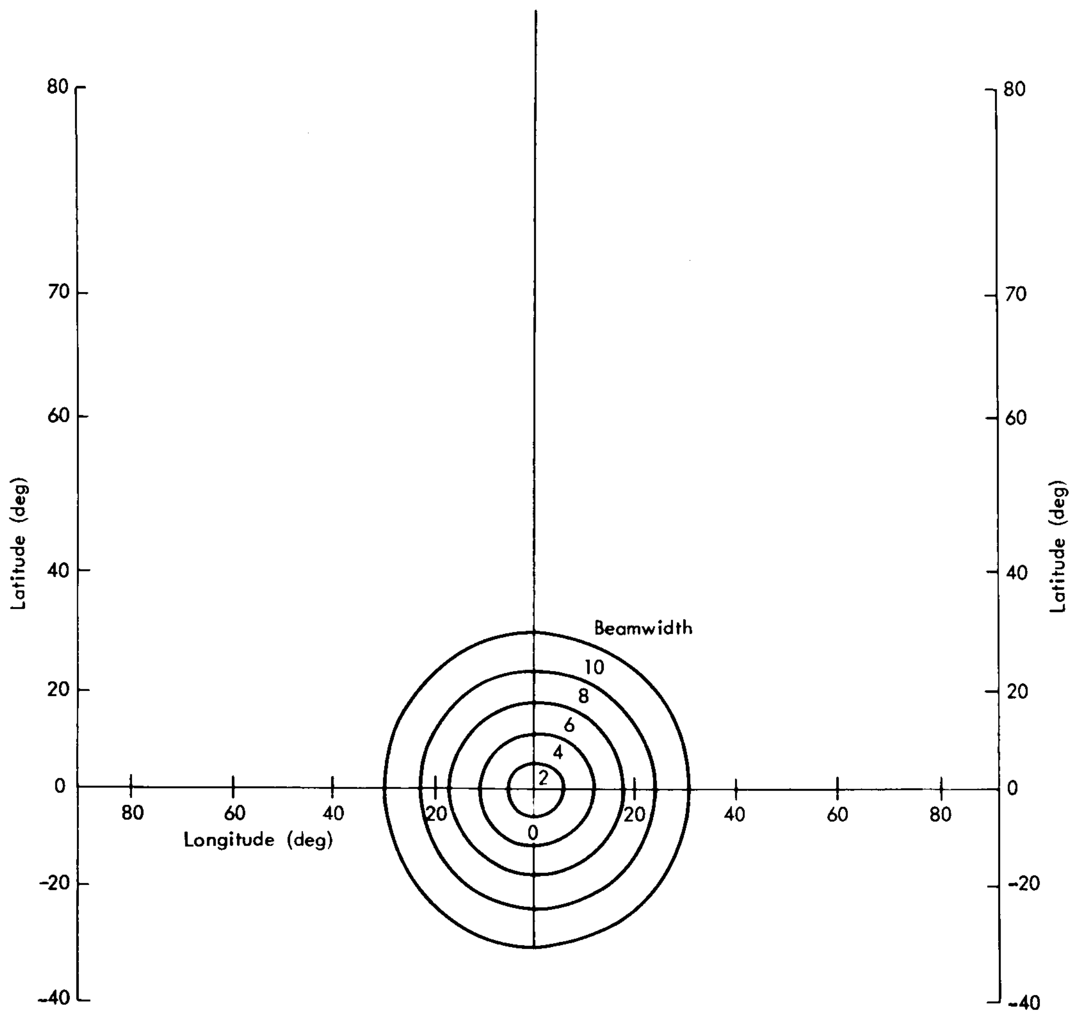

Fig. 17—Earth coverage patterns—offset angle 0°

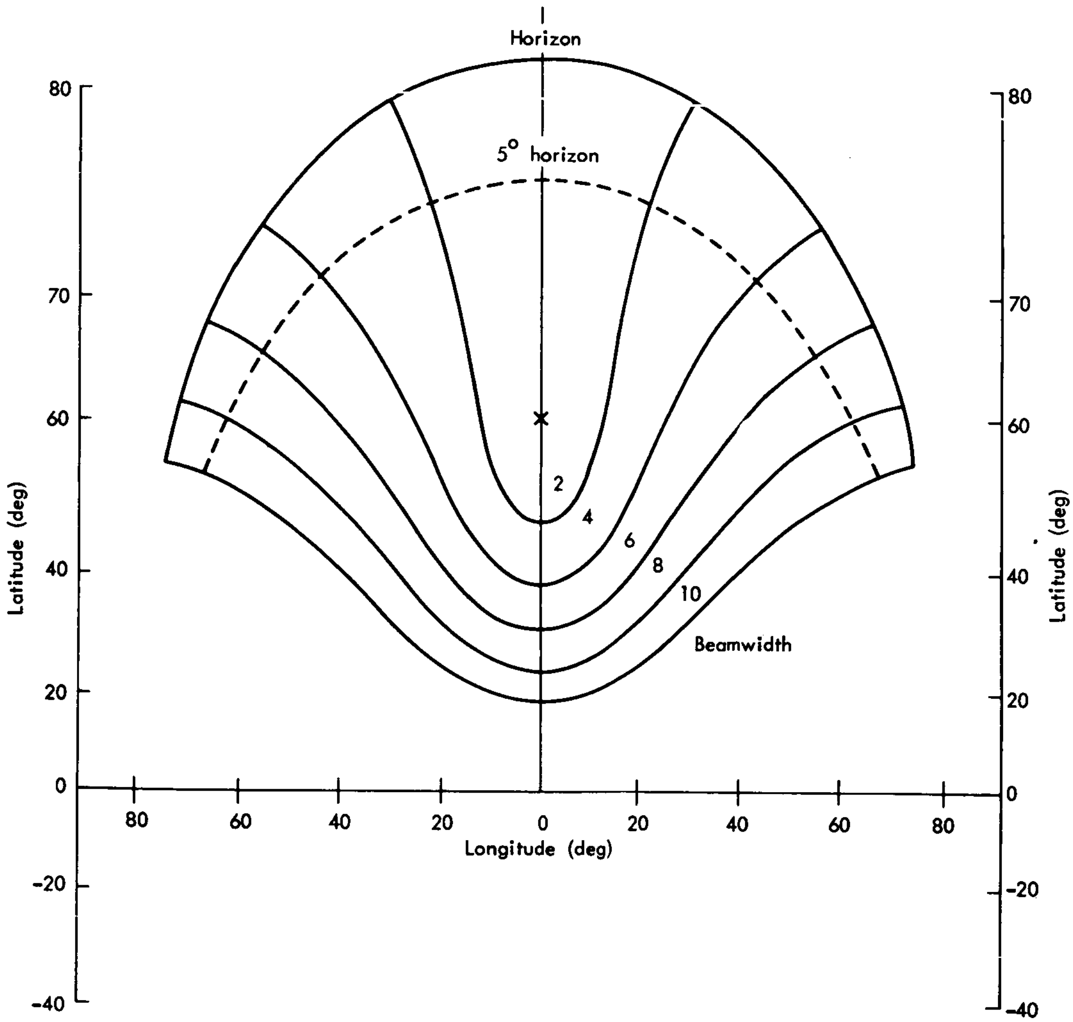

Fig. 18—Earth coverage patterns—offset angle—60°, —azimuth—90°

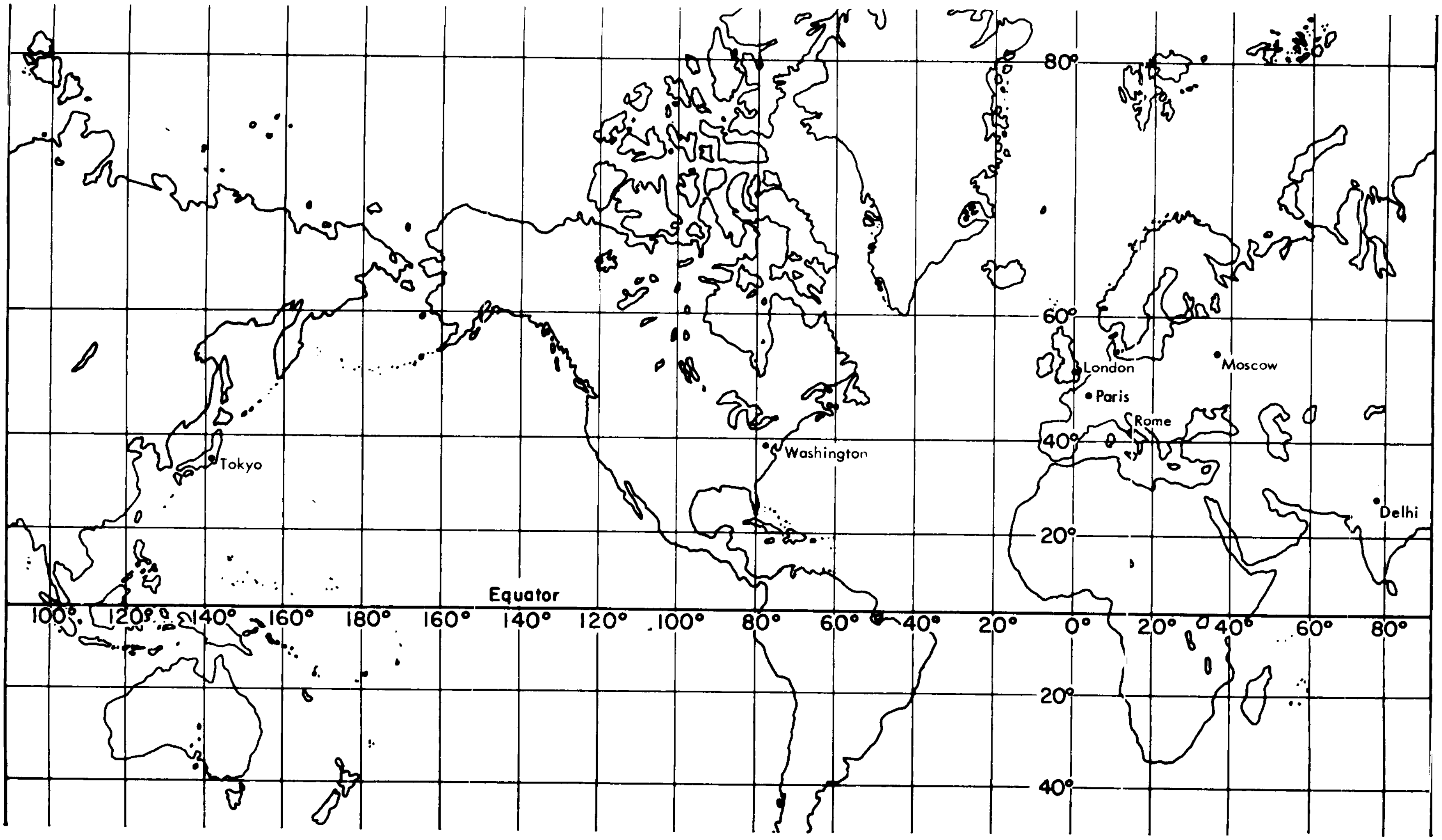

80°
60°
40°
20°
20°
40°
London
Paris
Rome
Moscow
Delhi
Washington
Tokyo
Equator
100°
120°
140°
160°
180°
160°
140°
120°
100°
80°
60°
40°
20°
0°
20°
40°
60°
80°